New Insight into the Role of Electron Transfer to O_2 in Photocatalytic Oxidations of Acetone over TiO_2 and the Effect of Au Cocatalyst

Baoshun Liu,*,[†] Hao Wu,[†] Xintong Zhang,[‡] Ivan P. Parkin,[§] and Xiujian Zhao[†]

[†]State Key Laboratory of Silicate Materials for Architectures, Wuhan University of Technology, Wuhan, Hubei 430070, People's Republic of China

[‡]Key Laboratory of UV-Emitting Materials and Technology of Chinese Ministry of Education, Northeast Normal University, 5268 Renmin Street, Changchun 130024, People's Republic of China

[§]Department of Chemistry, Materials Chemistry Centre, University College London, 20 Gordon Street, London WC1H 0AJ, U.K.
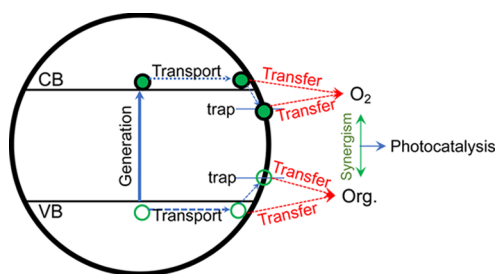
ABSTRACT: Photocatalytic oxidation by semiconductors is a dominant way to eliminate toxic organic pollutants. Different from thermal-activated catalysis, it is generally considered that the rate of charge carrier transfer from semiconductors to reactants determined photocatalytic activity. However, how charge carrier transfer correlates with photocatalytic activity is not well known, especially in gaseous photocatalytic oxidations of organics. By means of photoconductances, the present research gains some novel insight into the electron transfer in the acetone photocatalysis over TiO_2. Because it is shown that the electron transfer from TiO_2 to O_2 is faster than the acetone conversion, our results point

toward a fact that the electron transfer also contributes to the recombination via the O_2 sorption cycling in addition to the photocatalytic effect. The role of Au for a cocatalyst was also investigated in the acetone photocatalysis. It is found that the decoration of TiO_2 with Au nanoparticles indeed leads to an increase in the electron transfer from TiO_2 to O_2. Instead of a desirable increase, the photocatalytic rates however are decreased by Au decoration, independent on the methods to deposit Au, the Au nanoparticle size, and the Au amounts. The Au decoration also has no effect on the apparent activation energies of acetone conversion. These results lead to that the Au-induced increase in the electron transfer cannot contribute to the photocatalysis but can contribute to the recombination via the O_2 sorption cycling. Therefore, it is possible that the photoinduced holes tend to accumulate around the Au/TiO_2 perimeter and then recombine with the photoinduced electrons stored on Au at a faster rate, resulting in the decrease of photocatalytic activity. This research sheds some new light on the role of electron transfer in photocatalysis. The mere increase of the electron transfer could not promote the photocatalytic effect if the O_2 sorption-assisted recombination is not inhibited; this should be helpful in designing highly-efficient photocatalysts.
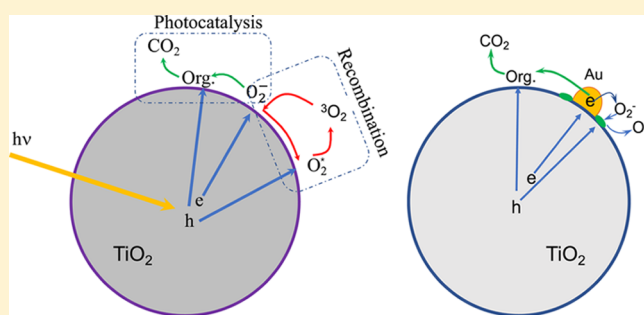
1. INTRODUCTION

Photocatalysis has received much attention over the past 50 years.[1] Much of the research has been driven by potential application of photocatalytic oxidations in eliminating toxic organics, which has advantages over thermocatalysis working at higher temperatures.[2−6] Semiconductor photocatalysis results from super bandgap light excitation.[7−9] As shown in Figure 1, electrons and holes are created and then go on to recombine or diffuse to the surface, where they are then transferred to adsorbed species such as molecule O_2, hydroxyl groups, and organic species for subsequent reactions.[10−12] Here, the holes and electrons can transfer to organics and electron acceptors, such as molecule oxygens, respectively, directly from the valence band (VB) and conduction band (CB) of semiconductors or indirectly assisted by surface traps.

The overall photocatalytic effect results from the synergism of the hole and electron transfer. Hole transfer must balance with electron transfer so as to sustain a continuous photocatalysis; this means that the slower process may limit the rate of a photocatalytic reaction.[13] Therefore, it has been actually taken as a basic rule throughout the literature to increase photocatalytic rates by increasing the slower steps of charge carrier transfer. The O_2 molecule is indispensable in gaseous photocatalytic oxidations of organics such as volatile organic compounds (VOCs). The electron transfer to O_2 from the photocatalyst will result in superoxide radicals ($\cdot O_2^-$) and other active oxidation species, responsive for many photo-

Figure 1. Diagram of kinetic process of the electrons and holes in semiconductor photocatalytic oxidations; the hole and electron transfer are shown in red fonts for clarification.

catalytic oxidations over TiO$_2$ and other materials.[14−17] Transient studies revealed that the kinetics of electron transfer from TiO$_2$ to O$_2$ is on the microsecond timescale; this is slower than the kinetics of hole transfer to organics, which is on the picoscale to nanoscale timescale.[18] This implies that the electron transfer to O$_2$ might limit many photocatalytic organic oxidations.[8,13,19] Increasing the kinetics of electron transfer is therefore considered to be important in increasing photocatalytic activity.

Therefore, many studies were carried out to modulate electron transfer of TiO$_2$ materials by using cocatalysts and defects, so as to increase photocatalytic activity.[20−24] Our phenomenologically theoretical analysis showed that the defect-derived gap states were good for increasing photocatalytic activity if electron transfer kinetics could be increased.[25] It has also been revealed that oxygen defects could act as the sites adsorbing O$_2$, as well as the sites accelerating the electron transfer from TiO$_2$ to O$_2$.[26,27] For example, we saw that the Au-induced oxygen defects could increase electron transfer from TiO$_2$ to O$_2$ and lead to an increase in methyl orange photocatalytic degradation.[28] It has been reported that oxygen defects created by hydrogen reduction of TiO$_2$ could lead to an increase in methylene blue photocatalytic degradation due to an increase in electron transfer.[29] Li et al. further suggested that tuning the distribution of oxygen defects on surfaces and in the bulk would result in a great increase in the photocatalytic oxidation of benzene over TiO$_2$.[30] Zhang et al. also thought that the photocatalytic oxidations of acetaldehyde over TiO$_2$ and WO$_3$ are sensitive to oxygen defects.[31,32]

Cocatalysts, such as Pt, Au, Cu(OH)$_x$, and others, have been used for promoting photocatalytic oxidations by increasing electron transfer from TiO$_2$ to O$_2$. For example, it has been reported that decoration of TiO$_2$ with Cu(OH)$_x$ nanoclusters could effectively increase photocatalytic oxidations of acetaldehyde over TiO$_2$ upon visible illumination due to the presence of multielectron transfer via Cu(OH)$_x$ nanoclusters.[33,34] Some studies have also reported that electron trapping by Pt may increase the rates of electron to O$_2$ on the Pt surface, increasing O$^-$ or $\cdot$O$_2^-$ species, which might participate in the attack on neighboring, adsorbed organics.[35,36] Trapping of electrons on Pt improved charge separation and may also aid photocatalytic oxidations by increasing hole lifetime through lowering electron−hole recombination rates.

Owing to a low work function,[37] Au has been used for a cocatalyst of TiO$_2$ for increasing the photocatalytic activity of TiO$_2$ materials because it could store electrons and mediate electron transfer. The high Schottky barrier between Au and TiO$_2$ (0.8 to 1 eV) could also prevent electrons from returning to TiO$_2$,[38] so the photoinduced holes and electrons are separated in distance and their lifetimes are prolonged. For example, upon UV light illumination, it has been reported that fast electron transfer from TiO$_2$ to Au led to a quick accumulation of long lifetime electrons.[39] The electrons can also transfer to O$_2$ at a faster rate due to the cocatalyst role of the Au nanoparticle; thus, decoration of TiO$_2$ with Au is thus hopeful in increasing photocatalytic activity.[40,41] For example, Yu et al. observed that decorating TiO$_2$ with Au could increase the rate of formaldehyde photocatalytic oxidations;[42] Kowalska et al. also reported that the photocatalytic oxidations of acetaldehyde over TiO$_2$ could be increased by Au decoration, almost independent of Au size and TiO$_2$ substrate types.[43]

However, although it is thought that the kinetics of electron transfer from TiO$_2$ to O$_2$ is important in photocatalytic oxidations of organics over TiO$_2$ due to its relatively slower kinetics and the decoration of TiO$_2$ with cocatalysts could increase photocatalytic activity through an increase in electron transfer,[44−47] how the electron transfer correlates with photocatalytic reactions is not well answered in the literature, especially for gaseous organic photocatalytic oxidations. Therefore, whether it could really limit a photocatalysis or still remains unknown. In addition to electron transfer, heterogeneous photocatalysis over TiO$_2$ also involves adsorption and desorption of reactants, as well as some intermediate steps following electron transfer, and in principle, each of them might limit photocatalysis.[36] Therefore, it is needed to first know the kinetics of electron transfer from TiO$_2$ to O$_2$ and then compare it with that of photocatalysis. This issue is interesting because it is in close relation to the kinetic nature of the photocatalytic oxidative mechanism. However, it is still a challenge to obtain the kinetics of electron transfer to O$_2$ due to an absence of suitable research methods.

In the current research, by means of electric conductances, the kinetics of electron transfer from TiO$_2$ to O$_2$ was studied and compared with the apparent kinetics of photocatalytic oxidations of acetone over TiO$_2$. Metal Au nanoparticles were also deposited on TiO$_2$ to study the role of cocatalysts. The effect of Au on the kinetics of electron transfer from TiO$_2$ to O$_2$ was studied and compared with that of acetone photocatalytic oxidations. The results led to a conclusion that, independent of Au deposition, electron transfer did not limit the whole acetone photocatalytic oxidation. Although Au deposition increased the kinetics of electron transfer, the rate of acetone photocatalytic oxidations showed an obvious decrease as compared to that of pure TiO$_2$, also independent on Au size and amount. This finding implies that the electron transfer from TiO$_2$ to O$_2$ also initiates other processes except for a photocatalytic effect. All experimental proofs pointed toward the recombination being mediated by O$_2$ sorption (adsorption−desorption) cycling on the TiO$_2$ surface. It seemed that Au-induced electron transfer might increase this recombination; hence, the acetone photocatalytic oxidation is thus decreased. Based on these findings, a diagram demonstrating kinetics of charge carriers and the relation to photocatalytic effects was developed.

2. EXPERIMENTAL SECTION

2.1. Materials and Au Decoration. *2.1.1. Pure TiO$_2$ Coatings.* A commercial paste made of P25 materials (HEPTACHROMA Company, Dalian, China) was fully coated on 40 mm × 20 mm quartz glass substrates to obtain several porous nanocrystalline (nc-TiO$_2$) coatings by the

doctor-blading method, which were then subjected to post-annealing at 450 °C for 2 h to remove organics and increase TiO_2 nanoparticle connection for the conductance measurement. The as-prepared TiO_2 coatings were directly used in photocatalytic experiments, conductance measurement, and Au sputtering without further treatment.

2.1.2. Au/TiO_2 Prepared by Photodeposition. The Au/TiO_2 material was prepared by means of photodeposition. Briefly, 1 g of P25 TiO_2 powder was dispersed in 70 mL of deionized water under stirring. Two milliliters of 10 g L^{-1} $HAuCl_4$ aqueous solution was then added. Ammonia solution was slowly dropped into the above solution until the pH reached ~9. The suspension solution containing both TiO_2 and $HAuCl_4$ was then illuminated with 365 nm UV light (3.6 mW/cm²) for 1 h while stirring to prepare the Au/TiO_2 samples. The Au/TiO_2 sample was then cleaned and filtered several times by water, which was then dried overnight for further use. The pure TiO_2 sample was prepared for comparison according to the same procedure without using $HAuCl_4$.

2.1.3. Sputtered Au/TiO_2 Coatings. Because the preparation of Au/TiO_2 by photodeposition used ammonia and $HAuCl_4$, their interaction with the TiO_2 surfaces may affect photocatalytic activities. Therefore, for comparison, the Au/TiO_2 material was also prepared by sputtering from a 99.99% Au target with a sputter coater (Cressington 108 Auto), which did not introduce any other impurities. A thin Au film was sputtered on the TiO_2 coatings and was then annealed in air to obtain the sputtered Au/TiO_2 samples. The power to sputter Au over the TiO_2 surfaces was kept at 45 W for the samples. Different times of sputtering were varied to change the amount of loaded Au nanoparticles. In addition, the samples prepared from 5 s sputtering were also subjected to different temperature post-annealing to modulate the size of Au nanoparticles.

2.2. Catalyst Characterization. The surface images of TiO_2 and Au/TiO_2 were observed with field emission scanning electron microscopy (FE-SEM; type: S-4800, Hitachi, Tokyo, Japan) and field emission transmission electron microscopy (TEM; type: JEM2100F, JEOL, Tokyo, Japan). The Au atomic contents of the Au/TiO_2 sample were determined by inductively coupled plasma (ICP-OES; type: Prodigy 7, LEEMAN LABS, USA) measurements. X-ray diffraction (XRD) patterns were collected with a grazing incidence X-ray diffraction (XRD; Empyrean, PANalytical, Almelo, Netherland) with the Cu Kα radiation being used as the X-ray source. The surface chemical composition of the Au/TiO_2 sample was checked with an X-ray photoelectron spectrometer (XPS; type: VG Multilab 2000, Thermo Scientific, Waltham, U.S.A.), with an X-ray source working with the Al Kα radiation using the binding energy (284.6 eV) of C 1s electrons as the energy reference. UV-vis-diffused spectra of the samples were measured by using a UV-vis photo spectrometer within a wavelength range from 200 to 800 nm (type: UV-3600, Shimadzu, Tokyo, Japan). The X-band electron paramagnetic resonance (EPR) spectra were recorded on a Bruker EMXnano spectrometer equipped with a cylindrical quartz tube operating at 100 kHz field modulation and a temperature of 100 K and room temperature in the dark and under 5 mW/cm² 365 nm monochromic light illumination.

2.3. Photocatalytic Experiments. Photocatalytic experiments were conducted in a self-designed pure quartz glass-closed circulation cylindrical batch reactor. A Pt100 resistance thermometer detector (RTD) connected with a temperature displayer was inserted into the middle of the reactor to monitor real reaction temperature. The photocatalytic reactor was heated to the set temperature by a heating plate. A mercury lamp (USHIO SP-9) equipped with a 365 nm band pass optical filter was used as the light source. The 365 light ensures that only the TiO_2 was excited, so the cocatalyst role of Au could be discussed. The light intensity was determined with a Si diode photodetector (Newport 843-R), which was kept at around 3 mW/cm⁻² for all of experiments. The temperature was varied between 20 and 80 °C with an interval of 15 °C.

The experiments were performed at constant temperature and air pressure. The samples were first pretreated under UV light illumination for ~24 h to remove residual carbonate contaminants before photocatalytic experiments. Clean air was flowing through the reactor for ~15 min to purge out the old air until the residual CO_2 concentration was lower than 20 ppm. The tightness of the photocatalytic reactor was evaluated by observing the change of CO_2 concentration in a blank experiment; this shows a very slow CO_2 leaking, so its effect on the photocatalytic activity was neglected.

Acetone was used as the VOC for photocatalytic oxidations. For the pure TiO_2 coatings and sputtered Au/TiO_2 coatings, three coated samples were placed in the photocatalytic reactor for photocatalytic reactions and the total amount of TiO_2 is ~0.015 g. For the photodeposited samples, 0.1 g of pure TiO_2 and Au/TiO_2 powders was dispersed ultrasonically with pure water in ϕ 50 mm glass containers. After removing the water by heating, a thin coating of the sample was formed on the bottom of the container and was used for the acetone photocatalysis. Before injecting acetone, the reactor containing the TiO_2 sample was kept in the dark for 30 min at the set temperature. Subsequently, 2 μL of liquid acetone was injected into the container, which was then kept in the dark for another 30 min to allow an adsorption−desorption dark equilibrium to be established. Then, the 365 nm UV light was switched on and illuminated the TiO_2 and the Au/TiO_2 samples for 30 min. The concentration of acetone and CO_2 was measured in line with a photoacoustic IR Multigas Monitor (INNOVA Air Tech Instruments Model 1412). The acetone conversions were fitted to a quasi-first-order kinetics to obtain the quasi-first-order constant. In addition, the CO_2 evolutions accord well with the zero-order kinetics, so its rate of CO_2 formation was also used to evaluate the photocatalytic activity.

2.4. Electric Conductance Measurement. Vacuum conductances were measured in a self-designed setup that contains an electrical conductance measurement part, a vacuum system, an atmospheric system, a temperature-controlling system, and a light source. The INSPEC electrical conductance-testing chamber containing a temperature-programmed sample platform was the main part. The top cover contains a piece of quartz glass to allow light illumination on the sample surface. The temperature was under accurate control between −190 and 450 °C by heating and a liquid N_2 cooling system.

For the samples obtained from photodeposition, 0.2 g of the above pure TiO_2 and Au/TiO_2 powder was mixed with water in a mortar, which was then ground for a while to obtain two sample pastes. Then, the TiO_2 and Au/TiO_2 pastes were coated on quartz glass substrates by a doctor-blading method, which was then heat-treated at 450 °C for 1 h. The samples of pure TiO_2 coatings and sputtered Au/TiO_2 coatings were directly used in the photoconductance measurements. Two
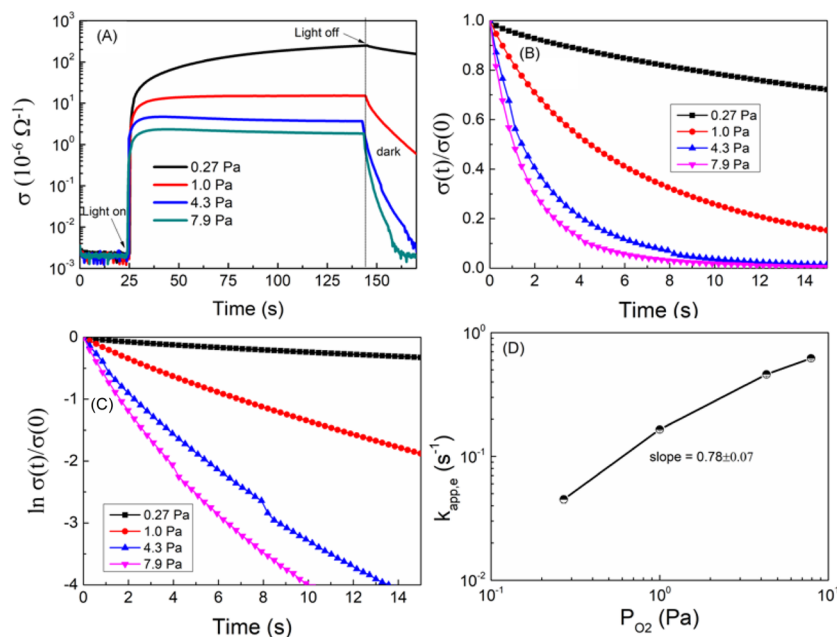
Figure 2. (A) Vacuum electric conductances of TiO_2 under modulation of light illumination at different P_{O2}'s and at room temperature ($\sim$25 °C). (B) Normalized transient photoconductances ($\sigma(t)/\sigma(0)$) at the different P_{O2}. (C) Dependences of $\ln(\sigma(t)/\sigma(0))$ on time at the different P_{O2}. (D) Log–log dependence of $k_{app,e}$ on the P_{O2}; ($\sigma(0)$ and $\sigma(t)$ denote the conductance at the time when the light illumination was turned off and the conductance after t seconds).

gold electrodes were sputtered on these coatings with a mask on the top, and a thin strip of coating (0.2 mm width) was kept out for UV light illumination (Figure S1). Afterward, the coatings were placed on a sample platform and the chamber was evacuated to below 1 mTorr by combining a mechanical pump and a molecular pump. The vacuum conductances at different temperatures and different O_2 partial pressures under simultaneous light illumination were measured with an electronic source meter (KEITHLEY 2450 Source Meter). A mercury lamp (USHIO SP-9) equipped with a 365 nm band pass optical filter was used to generate 365 nm monochromic light that did not lead to an increase in surface temperature.

In addition, the on-line electric photoconductances over the acetone photocatalysis were also measured in the same self-designed quartz reactor with a heating plate. Both the samples used for acetone photocatalysis and photoconductance measurements were put into the photocatalytic reactor, as shown in Figure S2. The Au electrodes were also prepared for the conductance measurement according to Figure S1. First, the mixture of N_2 (99.999%) and O_2 (99.999%) was flowed through the reactor for $\sim$15 min to purge out old air. The relative oxygen concentrations in these measurements were adjusted by changing the oxygen flow rate by keeping the nitrogen flow rate unchanged. The same 365 nm UV light was switched on to illuminate the samples. After 10 min of illumination, 2 μL of liquid acetone was injected into the reactor and the light illumination was kept on. The concentrations of acetone and CO_2, as well as the on-line conductances of the TiO_2 coating, were monitored during the whole procedure with a Photoacoustic IR Multigas Monitor (INNOVA Air Tech Instruments Model 1412) and the electronic source meter (KEITHLEY 2450 Source Meter). The electric photoconductances at air pressure were also measured at different relative O_2 concentrations without adding acetone.

3. RESULTS AND DISCUSSION

3.1. Electron Transfer from TiO_2 to O_2 and Its Relation to Photocatalytic Oxidation of Acetone. *3.1.1. Vacuum Photoconductance Analysis.* The electron paramagnetic resonance (EPR) results showed that the superoxide radicals ($\cdot O_2^-$) can be generated over the TiO_2 surface under super bandgap UV light illumination (Figure S3A,B); this shows that the electron transfer from TiO_2 to the molecule O_2 is present and should play an important role in photocatalysis of TiO_2 materials. Electric photoconductances were then further used to investigate the kinetics of electron transfer from TiO_2 to O_2. First, experiments were carried out in vacuum to measure photoconductances of TiO_2 as a function of O_2 partial pressure (P_{O2}) under modulation of UV light illumination, as shown in Figure 2A. In principle, although both the photoinduced electrons and holes can contribute to photoconductances, it was generally accepted that the photoinduced holes will be trapped at the surface and becomes immobilized for nano-TiO_2 materials, so the photoinduced electrons lead to photoconductances.[48] This is also supported by our data because the photoconductance decreases with the increase in the P_{O2}.

Photoconductances are determined by the change in photoinduced electron number and electron mobility. It has been reported that the electron mobility of some oxides such as nanostructural ZnO and SnO_2 is subjected to an increase upon light illumination.[49,50] The electron mobility of nano-TiO_2 was however reported to be insensitive to light illumination,[51,52] so the as-observed photoconductivity should be mainly caused by an increase in a free electron number. Upon light illumination, the electric conductances present a decrease with an increase in the P_{O2}; based on the EPR results (Figure S3), it can be known that this is in relation to the increase of electron transfer from TiO_2 to O_2 that would lead to a decrease in the number of electrons. Figure 2B shows the normalized transient conductances when the light was
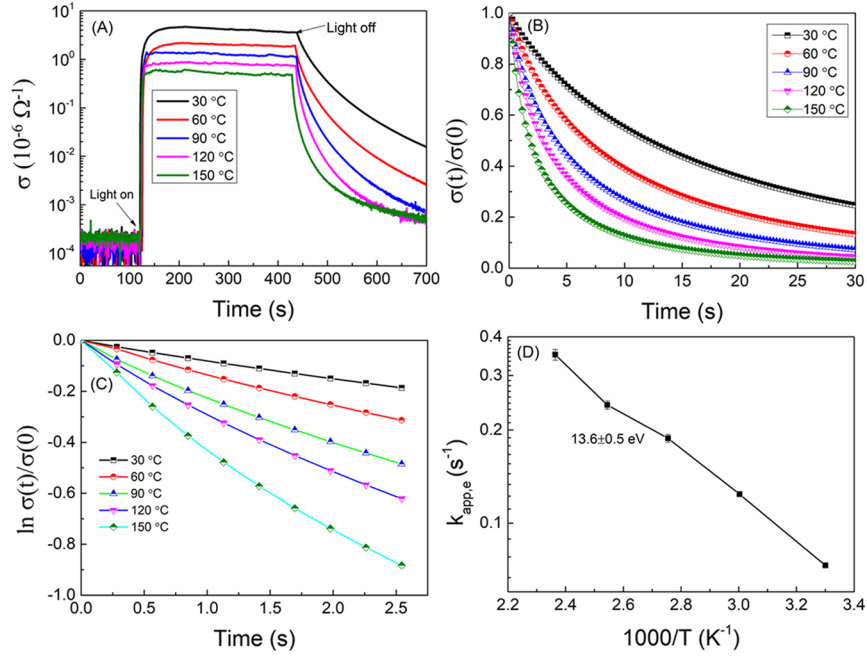
Figure 3. (A) Vacuum electric conductances of TiO₂ materials modulated by 365 nm light illumination at the oxygen partial pressure (P_{O2}) of 1.0 Pa and at different temperatures over 30 to 150 °C. (B) Corresponding normalized transient photoconductances ($\sigma(t)/\sigma(0)$) at the different temperatures. (C) Corresponding dependences of $\ln(\sigma(t)/\sigma(0))$ on time at the different temperatures. (D) Arrhenius dependence of the $k_{app,e}$ on the temperatures.

switched off; the time at which the light was turned off was set as zero. The decay rates of photoconductances increase as the P_{O2} increases, implying that the electron transfer to O₂ is a dominant route to remove the photoinduced electrons in TiO₂. The transient photoconductances indicate that the electron number is subjected to a dynamic decrease due to electron transfer to O₂, so they can be used to study the kinetics of electron transfer from TiO₂ to O₂.

As shown in Figure 1, the photoinduced electrons can transfer to O₂ via the CB and surface traps. Here, we do not consider the detailed kinetics of electron transfer. Irrespective of electron transfer kinetics, directly via the CB states or indirectly via the surface traps, under the consideration of single-electron transfer, the rate of electron transfer to O₂ could be described as

$$r(t) = \frac{dn(t)}{dt} = k_e[O_2]n(t) = k_{app,e}n(t) \tag{1}$$

where k_e and $n(t)$ denote the rate constant of electron transfer and free CB electron number at time t, respectively. If the n at the time when the light illumination was powered off is taken as $n(0)$, this formula can be transferred to the following equation.

$$\ln \frac{n(t)}{n(0)} = k_{app,e}t \tag{2}$$

where $k_{app,e}$ is the product of k_e and $[O_2]$, defined as the apparent rate constant of electron transfer. As the $n(t)$ is proportional to the conductance at time t, this formula can be written as

$$\ln \frac{\sigma(t)}{\sigma(0)} = k_{app,e}t \tag{3}$$

Figure 2C shows the dependence of $\ln(\sigma(t)/\sigma(0))$ on time at different P_{O2}'s. The electron transfer to O₂ cannot be fully described by first-order kinetics, indicating that the electrons captured by adsorbed O₂ might not be in equilibrium with gaseous O₂ or be involved in several kinetics; this is also in line with other studies.[53] The slopes of the beginning of these plots (from 0 to 4 s) were obtained to represent $k_{app,e}$. Figure 2D shows the log−log dependence of the $k_{app,e}$ on the P_{O2}. It is seen that the $k_{app,e}$ depends on the P_{O2} in a sublinear mode ($k_{app,e} \propto P_{O2}{}^{\alpha}$) with an index ($\alpha$) of 0.78. This implies that the electron transfer from TiO₂ to O₂ is possibly dependent on the ionosorption type of O₂ on the TiO₂ surface (O⁻ or O₂⁻).[54] Because the O₂ concentration is four to five orders of magnitude lower than that in air, the kinetic constant (k_e) of electron transfer to O₂ is determined to be on the microsecond timescale, in good agreement with that obtained from transient absorption studies.[55]

To check whether the electron transfer from TiO₂ to O₂ is dependent on temperatures, the vacuum photoconductances were also measured at different temperatures under a constant P_{O2}, as shown in Figure 3A. Upon UV light illumination, the photoconductances show a decrease with an increase of temperature. Figure 3B shows the normalized transient photoconductances at different temperatures. On the basis of the above analysis, this shows that the electron transfer from TiO₂ to O₂ belongs to a thermal process that increases with temperatures. This is also in good accordance with our previous study and a theoretical analysis.[56,57] The dependences of $\ln(\sigma(t)/\sigma(0))$ on time are shown in Figure 3C, based on which, the first-order rate constants ($k_{app,e}$) of the electron transfer are obtained and plotted in Figure 3D in the Arrhenius mode. The apparent activation energy of the electron transfer from TiO₂ to O₂ was calculated as 13.6 ± 0.5 kJ/mol. The heat-induced desorption of O₂ from the TiO₂ surface could not
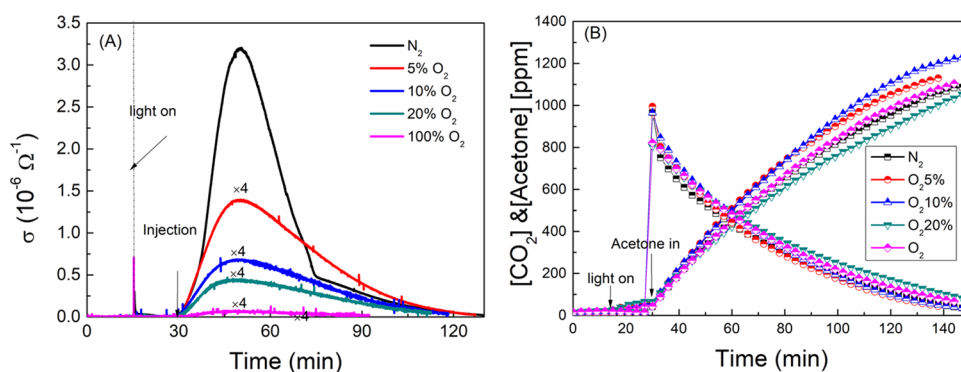
Figure 4. (A) Air pressure on-line photoconductances of TiO_2 during the photocatalytic oxidation of acetone in the presence of different relative O_2 concentrations and at a temperature of 50 °C. (B) Corresponding time dependences of CO_2 and acetone concentrations during the photocatalytic oxidations over TiO_2.
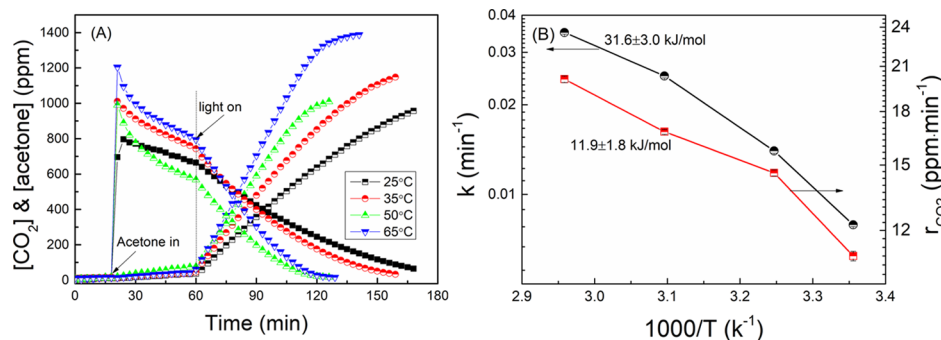
Figure 5. (A) Time dependences of CO_2 and acetone concentrations during the photocatalytic oxidations over TiO_2 in air at different temperatures and under 3 mW/cm² of 365 nm monochromic light illumination. (B) Corresponding Arrhenius phots of the rate constant of acetone conversion at different temperatures.

have a great effect on the kinetics of electron transfer, because it happens at temperature higher than 150 °C.[58,59]

3.1.2. On-Line Air Pressure Photoconductances and Photocatalytic Activities. On-line photoconductances along with acetone photocatalytic oxidations were also carried out under air pressure as a function of relative O_2 concentrations. To see the effect of acetone addition on photoconductances, experiments were carried out by injecting acetone with light illumination. Figure 4A shows the dependences of photoconductances on time as a function of relative oxygen concentrations. The photocatalytic oxidation of acetone led to a great increase of photoconductances in a N_2 atmosphere, implying that acetone photocatalysis is first initiated by hole transfer. The capturing of holes by acetone increased the number of electrons by reducing recombination. The increase in relative oxygen concentrations leads to an obvious decrease in photoconductances due to the increase of electron transfer. However, as shown in Figure 4B, the rates of acetone conversion and CO_2 evolution are almost the same for all relative oxygen concentrations, which is also in line with the observation of ref 51, because acetone photocatalysis is initiated by hole transfer. The increase of electron transfer ($k_{app,e}$) cannot contribute to the increase of the photocatalytic activity as expected. The presence of photocatalytic activity in a N_2 atmosphere is ascribed to the residual O_2. How the variation of relative oxygen concentrations affects electron transfer and photocatalysis is related to the change in electron numbers.

The on-line photoconductances show that the kinetics of electron transfer is slower than the hole transfer to acetone.

The above results also mean that the slower electron transfer could not limit the acetone photocatalysis. To further confirm this result, photocatalytic experiments were also carried out at different temperatures. The changes of acetone and CO_2 concentration in the course of acetone photocatalysis are shown in Figure 5A. The increase of CO_2 evolution rates with temperatures shows that the acetone photocatalysis contains a thermal process. Acetone conversions follow quasi-first-order kinetics. The rate constants were plotted as a function of temperatures in the Arrhenius mode, as shown in Figure 5B. The apparent activation energy of acetone conversions was determined to be 31.6 ± 3.0 kJ/mol, much higher than that of electron transfer (13.6 ± 0.5 kJ/mol). This undoubtedly confirms that the electron transfer from TiO_2 to O_2 should not limit the acetone photocatalysis although it is indispensable. The electron transfer must contribute to the other process in addition to the photocatalytic effect, so increasing the speed of electron transfer does not naturally lead to an increase in photocatalytic activity, as shown in Figure 4B. In addition, the CO_2 evolution apparently follows zero-order kinetics. The Arrhenius dependences of the CO_2 evolution rates on temperatures are also shown in Figure 5B (red line, right y axis). The apparent activation energy was determined to be 11.9 ± 1.8 kJ/mol, which is much lower than that of acetone conversion (31.6 ± 1.8 kJ/mol). Therefore, the acetone conversion does not lead to direct CO_2 evolution but requires some intermediate steps.

The dark adsorption of the acetone molecule over the P25-coating surface was determined by comparing the time dependence of acetone concentration. The specific surface

area of P25 coating is about 30 m^2/g and the volume of the photocatalytic reactor is about 1.0 L. The surface coverage of acetone over the TiO_2 surface is estimated by comparing the difference in time dependences of acetone concentration in the presence and absence of TiO_2 samples, as shown in Figure S4. The surface acetone coverage is determined to be $\sim5.0 \times 10^{-3}$ molecule/nm^2. As compared to formic acid and formaldehyde, the adsorbed capacity of acetone over the TiO_2 surface is much lower. However, the low adsorbed coverage of acetone could not limit the photocatalytic acetone conversion, because it is found that the photocatalytic rate linearly increases with light intensity, as shown in Figure S5. Therefore, the acetone photocatalytic conversion should be limited by a subsequent step following the electron transfer.

3.1.3. Parallel Role of Electron Transfer from TiO_2 to O_2. Then, a problem rises that what is the exact kinetic role of electron transfer in photocatalysis. The above result showed that the photoinduced holes can react with an acetone molecule over a shorter time and electron transfer to O_2 is slower. In the presence of acetone, the electrons accumulated in the CB, which contribute to the on-line photoconductances (Figure 4A) and have no counterparts to recombine with. The only way is to react with an acetone molecule (or intermediate species) that has already captured the holes. Because the synergism between the holes and electrons leads to a photocatalytic oxidation of acetone, dependent on the hole transfer rate, the electrons are accumulated to balance the hole transfer according to the following equation

$$k_{h}p[C_3H_6O] = k_{e}n[O_2] \tag{4}$$

where k_h and p are the hole transfer constant and hole concentration, respectively. The hole transfer to organics such as methanol, ethanol, and isopropanol are on the femtosecond to picosecond timescale.[60] Our previous study has shown that the number of accumulated electrons is much higher for methanol and formic acid photocatalytic oxidation.[56] Therefore, the rate constant (k_h) of hole transfer should be several orders of magnitude faster than that of electron transfer (k_e, on the microsecond timescale). The above result also indicates that acetone conversion should be controlled by an intermediate step after hole transfer due to its higher apparent activation energy. Therefore, the change in oxygen concentrations cannot have an obvious effect on the photocatalytic activity. The number of passivated electrons is varied inversely as a function of $[O_2]$ to balance the hole transfer according to eq 4.

In the absence of acetone, there is no hole transfer to organics (lefthand of eq 4). Figures 2A and 3A show that the electron transfer to O_2 still exists. Because the photocatalytic effect is absent in this case, the electron transfer to O_2 must contribute to recombination with holes trapped on the surface. Under gaseous conditions, the electron transfer could lead to an adsorption of O_2 on the TiO_2 surface. The resulting $\cdot O_2^{-}$ could react with the holes to form singlet-like O_2 (O_2^{*}).[61] Although O_2^{*} is also an active oxygen species, our result shows that it is incapable of oxidizing acetone as CO_2. O_2^{*} quickly relaxes to triplet ground-state O_2 and losses its oxidization ability before reacting with acetone. Finally, the O_2 desorbs from TiO_2 surfaces and can then participate in electron transfer and start a new recombination cycle. This is named as the recombination mediated by O_2 sorption (adsorption−desorption) cycling according to following equations.

$$O_2 + e \rightarrow O_2^{-} \tag{5}$$

$$O_2^{-} + h \rightarrow O_2^{*} \tag{6}$$

$$O_2^{*} \rightarrow O_2 \tag{7}$$

Therefore, the electron transfer from TiO_2 to O_2 simultaneously contributes to two parallel processes, the photocatalytic process (eq 4) and recombination (eqs 5−7). Based on the above discussion, the kinetic process of electron transfer is depicted in Figure 6.
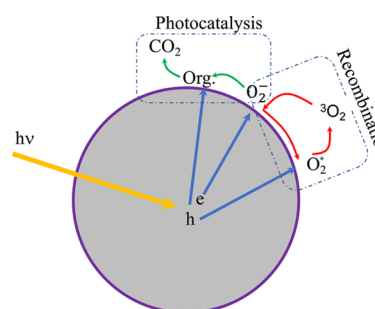

Figure 6. Diagram of electron transfer process in the gaseous photocatalytic oxidation of organics over TiO_2 material.

3.2. Effect of Au Deposition on Electron Transfer and Photocatalytic Activities.

3.2.1. Characterization of TiO_2 and Au/TiO_2 Sample Prepared by Photodeposition. XRD patterns and Raman spectra show that the Au/TiO_2 materials prepared by photodeposition and the corresponding pure TiO_2 are composed of rutile and anatase phases (Figures S6 and S7) and do not reveal the existence of Au due to the low amount. The morphology of the TiO_2 material, as observed by FE-SEM, is also unaffected to Au deposition. In addition, Au decoration also has a less effect on the specific surface area, which was measured to be 41 and 43 m^2/g for the pure and Au/TiO_2, respectively. The atomic amount of Au in the Au/TiO_2 was measured to be 0.15 at % by ICP-OES. Figure 7A shows the TEM image of Au/TiO_2 samples, which contains small Au spherical nanoparticles (labeled with red circles) in addition to the interconnected TiO_2 nanoparticles. Figure 7B shows the high-resolution TEM image of Au/TiO_2. The crystalline facets show the presence of anatase TiO_2 and Au nanoparticles. The spherical Au nanoparticle was shown to be in good connection with the anatase TiO_2 nanoparticles.

To see the valence states of Ti, O, and Au, the core-level XPS spectra were recorded. The Au deposition has a less effect on both O 1s and Ti 2p XPS spectra (Figure S8A,B). The Au 4f spectra of Au/TiO_2 are shown in Figure 8A. The Au 4f peak is asymmetrical due to the presence of both metal Au and Au^{3+}.[62] The relative amount of Au^{3+} was determined to be $\sim40\%$. The UV−visible diffusion spectra of the pure TiO_2 and Au/TiO_2 samples are shown in Figure 8B. The transmittance spectrum of the 365 nm band pass optical filter was also shown because it was used in the photocatalytic experiments. The pure TiO_2 and Au/TiO_2 have similar diffusion spectra except that the Au/TiO_2 sample presents a wide localized surface plasmonic resonance (LSPR) absorption around 560 nm,[63] which shows the existence of metal Au nanoparticles and is in good agreement with the XPS analysis. A wavelength of 365 nm light does not overlap with the LSPR absorption of Au nanoparticles, so it is not needed to consider the effect of
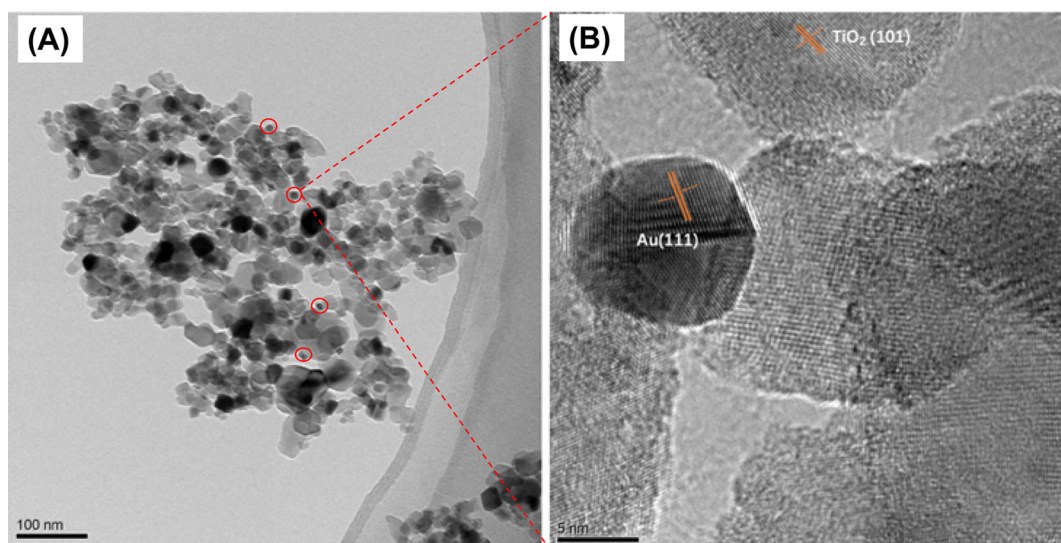
Figure 7. (A) TEM image and (B) high-resolution TEM images of the Au/TiO₂ materials.
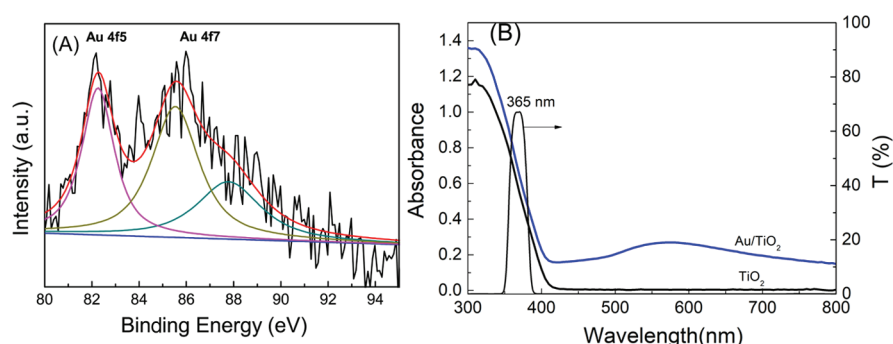
Figure 8. (A) Au 4f core-level high-resolution XPS spectrum of the Au/TiO₂ material. (B) UV−vis diffusion spectra of the TiO₂ and Au/TiO₂ materials; transmittance spectra of 365 nm band pass optical filter.

LSPR on photocatalysis, which ensures that the sole role of Au NPs as cocatalysts is studied.

3.2.2. Photocatalytic Activities and Apparent Activation Energies. Figure 9A shows the variations of acetone and CO_2 concentrations during the photocatalysis over the Au/TiO₂ and the corresponding pure TiO₂ at 30 °C. Both the rates of acetone conversion and CO_2 evolutions are faster for the pure TiO₂ than the Au/TiO₂. Because they have similar specific surface area and morphologies, the decrease in photocatalytic activity is tentatively assumed to be due to Au. Upon UV light illumination, the photoinduced conversions of acetone follow quasi-first-order kinetics and the initial evolutions of CO_2 follow the zero-order kinetics. The rate constants (k) of acetone conversions and the initial speeds of CO_2 evolution are shown in Figure 9B; these indicate the decrease of photocatalytic activity after Au deposition.

To check whether the Au deposition could affect the pathway of photocatalysis, photocatalytic experiments were also carried out at different temperatures (Figures S9 and S10). The quasi-first-order rate constants of acetone conversions over the pure TiO₂ and Au/TiO₂ were plotted in the Arrhenius way, as shown in Figure 9C. The apparent activation energy of acetone conversion over the TiO₂ is almost the same to that of the Au/TiO₂. The Arrhenius dependences of the rates of CO_2 evolution on temperatures are also shown in Figure 9D. The obtained apparent activation energy is almost the same for the TiO₂ and Au/TiO₂. The difference in the apparent activation

energy of acetone conversion and CO_2 evolution shows that the acetone photocatalysis over the Au/TiO₂ also does not directly lead to CO_2 evolution but needs some intermediated steps. Because both the apparent activation energies are the same for the TiO₂ and Au/TiO₂, it is thought that the Au does not change the pathway of acetone photocatalysis over TiO₂. Therefore, it was concluded that the photocatalysis does not happen around the Au/TiO₂ perimeter sites and on the Au surface but on the TiO₂ surface. Figure 9A,B also shows that all the photocatalytic activities of the Au/TiO₂ are lower at all temperatures compared to TiO₂.

3.2.3. Effect of Au on the Electron Transfer from TiO₂ to O₂. To determine the effect of Au on the electron transfer from TiO₂ to O_2, electric photoconductances were measured in vacuum at different temperatures. Figure 10A,B show that the photoconductances of Au/TiO₂ are obviously lower than that of pure TiO₂ upon light illumination. The photoconductances measured at 30 °C are also shown in Figure 11A to give a clear comparison. It is seen that the photoconductance of the Au/TiO₂ is lowered by the increase of electron transfer after Au deposition, as revealed by the normalized transient photoconductances (inset). The semi-log time dependences of the normalized transient photoconductances are shown in Figure 10C,D for the pure TiO₂ and Au/TiO₂, respectively. The transfer of electrons from TiO₂ to O_2 did not agree well with first-order kinetics because the electron transfer to O_2 cannot keep in equilibrium with O_2 adsorption−desorption. The
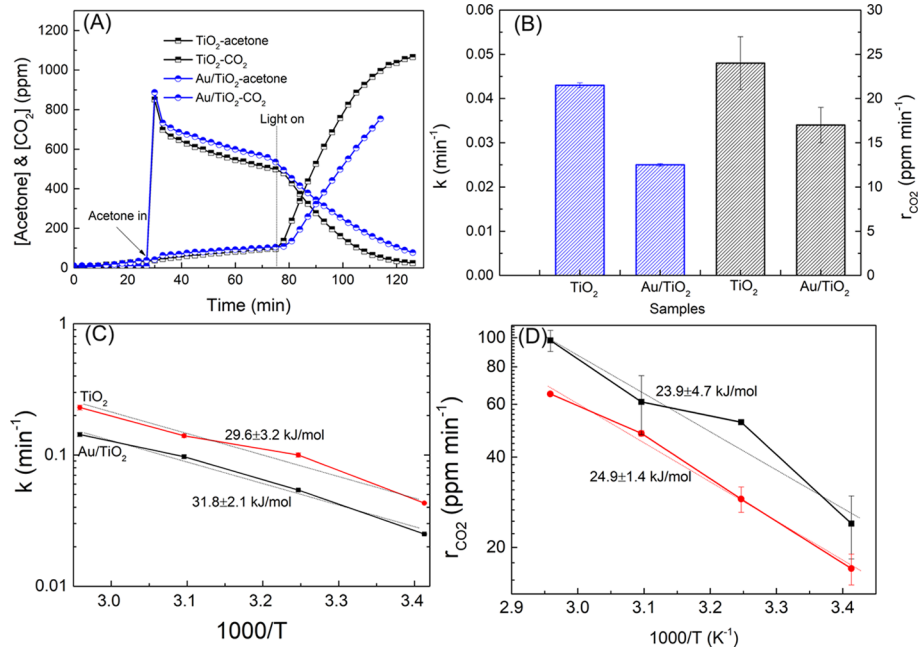
Figure 9. (A) Time dependences of acetone and CO_2 concentrations in the course of acetone photocatalysis over TiO_2 and Au/TiO_2 at a temperature 30 °C. (B) Quasi-first-order rate constants of acetone decomposition and initial speed of CO_2 evolutions. (C) Arrhenius plots of acetone photocatalytic decomposition over the TiO_2 and the Au/TiO_2 prepared from photodeposition method. (D) Arrhenius plots of initial CO_2 evolutions from the acetone decomposition over the TiO_2 and the Au/TiO_2 materials.
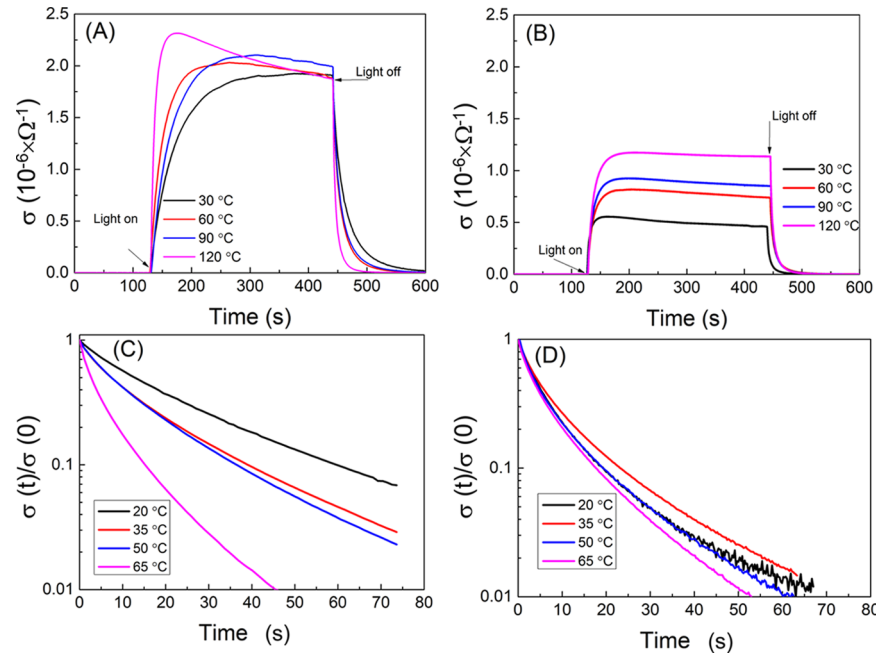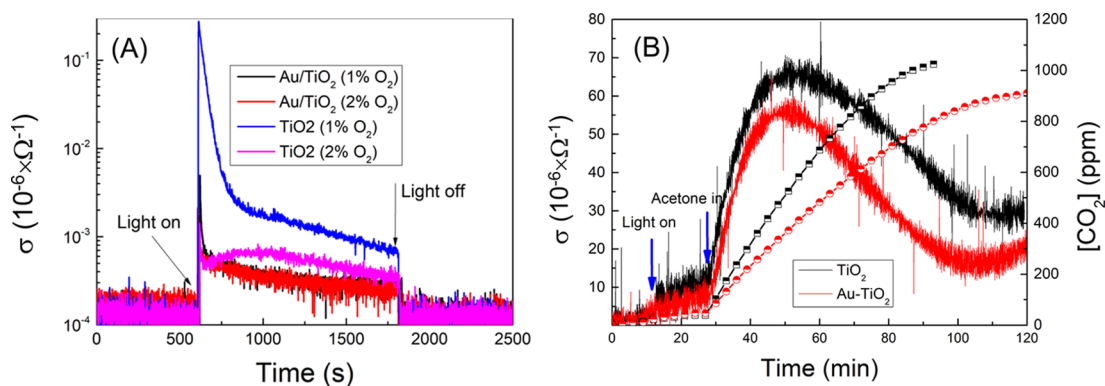

Figure 10. (A) Vacuum photoconductances of the pure TiO_2 at different temperatures under constant light intensity (3 mW/cm^2) and oxygen partial pressures (5.0 Pa). (B) Vacuum photoconductances of the Au/TiO_2 material prepared by photo deposition under the same conditions. (C) Semi-log time dependences of the normalized transient conductances of the pure TiO_2. (D) Semi-log time dependences.

increase of temperatures had a greater effect on the transient photoconductances of the pure TiO_2 than on Au/TiO_2. The rate constants (k) of electron transfer were obtained from the initial slopes (from 0 to 4 s) of these log time plots. The Arrhenius dependences of these rate constants are then shown in Figure 11B, based on which the apparent activation energy of the electron transfer from TiO_2 to O_2 was determined. It is seen that the apparent activation energy of the electron transfer from TiO_2 to O_2 is decreased more than six times by Au

deposition, so this reveals that the Au could act as an intermediate mediator bridging the electron transfer between TiO_2 and O_2, agreeing well with the recognition that Au belongs to a kind of electron cocatalyst.[42,43] It is also seen that the E_{app} of the pure TiO_2 here is higher than that of the TiO_2 material in section 3.1; this shows that the treatment of the TiO_2 material in the preparation solutions might change its surface structure and has a direct influence on the electron transfer kinetics.
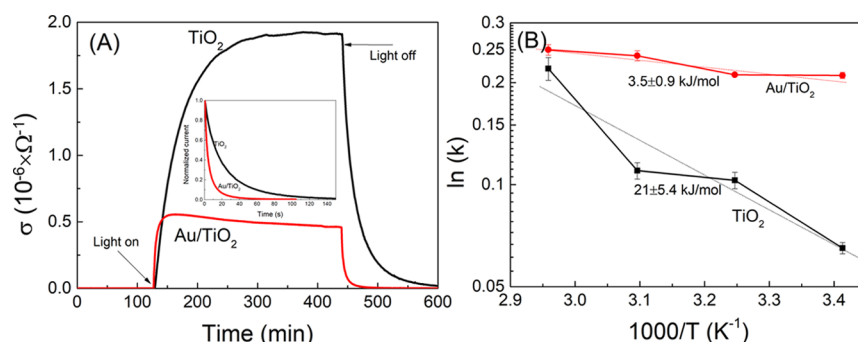
Figure 11. (A) Vacuum photoconductances of the pure TiO_2 and Au/TiO_2 prepared from photodeposition at the P_{O_2} of 4.0 Pa (light intensity: 2 mW/cm^2, temperature : 30 °C). (B)Arrhenius plots of the rate constants of the electron transfer for pure TiO_2 and the Au/TiO_2 prepared from photodeposition.

Figure 12. (A) Photoconductances of the TiO_2 and the Au/TiO_2 materials under UV light illumination measured air pressure containing 1 and 2 vol % oxygens. (B) On-line photoconductances of the pure TiO_2 and the Au/TiO_2 under UV light illumination in normal synthetic air in the absence and presence of acetone.

The photoconductances were also measured at air pressure by controlling the relative volume concentration of O_2 in a synthetic air. Figure 12A shows the photoconductances of the pure TiO_2 and Au/TiO_2 in air containing 1 and 2 vol % O_2. The photoconductance of the pure TiO_2 is higher than that of the Au/TiO_2. The transient photoconductances cannot be compared due to a fast electron transfer to O_2. As revealed above, because the photoconductances are mainly determined by electron transfer from TiO_2 to O_2, the lower photoconductances of the Au/TiO_2 mean the faster electron transfer, agreeing well with the vacuum conductance analysis. In the presence of 1 vol % O_2, just after light illumination, it is seen that the photoconductances show a sharp increase and a subsequent decrease for both the TiO_2 and Au/TiO_2 due to the fast generation of electrons by light illumination and the subsequent relatively slow transfer to O_2. The slower electron transfer from the pure TiO_2 to O_2 leads to a sharp increase as compared to the Au/TiO_2. The promotion of electron transfer by Au accelerates the balance between the electron photogeneration and the electron transfer to O_2, resulting in a lower increase in photoconductances.

Figure 12B shows the effect of acetone addition on the photoconductances of the pure TiO_2 and Au/TiO_2 in normal air; the CO_2 evolutions are also shown for comparison. It is seen that the addition of acetone increases the photoconductances of the TiO_2 and Au/TiO_2, along with the generation of CO_2. The photoconductances fall back to background values when the acetone was almost consumed. This result is in good agreement with Figure 4A, so the acetone

photocatalysis over the Au/TiO_2 also initiates from the hole transfer from TiO_2 to acetone. It is seen that the photoconductance of the pure TiO_2 is higher than that of the Au/TiO_2 due to a slower electron transfer to O_2. As the acetone photocatalysis first initiates from the hole transfer, the Au-induced decrease of photocatalytic activity should be ascribed to the increase in recombination that reduces the number of photoinduced holes.

3.2.4. Role of Au in Increasing the Recombination via the Photoassisted O_2 Adsorption/Desorption. Both the vacuum and air-pressure photoconductances revealed that the kinetics of electron transfer from TiO_2 to O_2 could be increased by Au; this however did not lead to a desired increase but a decrease in the acetone photocatalysis. The E_{app} of acetone conversion is completely different from that of the electron transfer (Figure 9C,D vs Figure 11B), so the electron transfer from TiO_2 to O_2 cannot be thought as the limited step of whole acetone photocatalysis, independent of Au deposition. The conventional standpoint indicates that the promotion of electron transfer to O_2 should be good for photocatalysis due to the separation of electrons and holes and the generation of more · O_2^- radicals; this is also often referred to a general rule to prepare of highly active photocatalysts. Because the electron transfer from TiO_2 to O_2 also contributes to recombination in addition to the photocatalytic effect, we thought that Au may increase recombination and thus result in a decrease in photocatalytic activity.

Because of the etching effect, the addition of $HAuCl_4$ might have an effect on the surface structure of TiO_2 and result in a
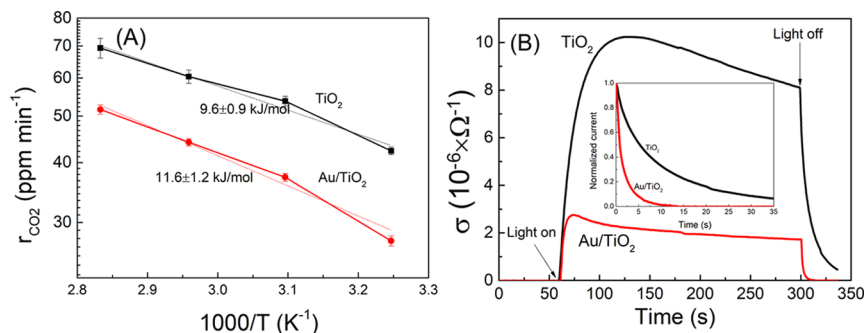
Figure 13. (A) Arrhenius plots of initial CO_2 evolutions from the acetone decomposition over the TiO_2 and the Au/TiO_2 materials. (B) Electric currents of the pure TiO_2 and Au/TiO_2 prepared thermal deposition method under 3 mW/cm^2 365 nm light illumination and 1.0 Pa P_{O_2} at 30 °C.

decrease in photocatalytic activity. To rule out this effect, the acetone photocatalytic experiments on the sputtered Au/TiO_2 (5 s sputtering and 450 °C) and the pure TiO_2 were also carried out at different temperatures. The pure TiO_2 used here was the same as that used in subsection 3.1. The sputtered Au/TiO_2 also presents a clear surface-localized plasmonic absorption, showing the existence of Au in the form of nanoparticles. The Arrhenius dependences of the CO_2 evolution rates on temperatures are shown in Figure 13A. This also shows that the acetone photocatalysis is decreased by Au over all studied temperatures. The Au deposition also has no effect on the E_{app} of the CO_2 evolution. Figure 13B shows the photoconductances of the pure TiO_2 and Au/TiO_2. It can be seen that the photoconductance of Au/TiO_2 is lower than that of the pure TiO_2. This is due to an increase in electron transfer to O_2 by Au, as revealed by the faster transient photoconductances (inset). Based on the above analysis, we concluded that the Au-induced decrease of acetone photocatalysis should result from an increase in the recombination mediated by O_2 adsorption−desorption cycling.

Recent studies showed that the Au/TiO_2 perimeter might prefer to trap photoinduced holes.[64] In this case, the electrons transferring to Au nanoparticles can easily recombine with the holes trapped at the Au/TiO_2 perimeter via O_2 adsorption−desorption cycling, as shown in Figure 14. Since Au decoration
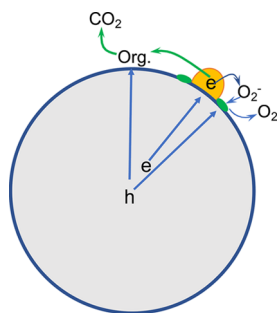

Figure 14. Diagram for the role of decorated Au NPs for accelerating the O_2 adsorption−desorption cycled recombination.

has no effect on the E_{app} of the acetone photocatalysis, the holes trapped at the Au/TiO_2 perimeter could not contribute to the photocatalysis because they are quickly removed by this kind of recombination or because the acetone molecules are not favored to be adsorbed at the Au/TiO_2 perimeter. The photocatalytic oxidations of acetone over Au/TiO_2 should mainly happen on the TiO_2 surface, so the photocatalytic pathway is the same as that of pure TiO_2. Therefore, the holes

trapped at the TiO_2 surface dominantly contribute to acetone photocatalysis, while those trapped at the Au/TiO_2 perimeter might mainly go to promote recombination, so the Au catalyzes the O_2 adsorption−desorption recombination in gaseous acetone photocatalytic oxidations (Figure 14).

The effect of loading amount and size of Au nanoparticles on the photocatalytic activity of sputtered Au/TiO_2 was also studied. The sputtering time was varied to change the Au nanoparticle loading amount. The UV−vis transmittance spectra (Figure S11A) of the Au/TiO_2 samples clearly show the increase of Au amount with the increase of sputtering time. The ICP analysis further shows that Au/Ti ratios are 4.02 %, 7.5%, and 11.4%, respectively, after sputtering Au for 5, 10, and 15 s, respectively. In addition, the UV−vis transmittance spectra (Figure S11B) of Au/TiO_2 show the increase of plasmon absorption with the post-annealing temperature, indicating the increase of the Au nanoparticle size; this is also confirmed the TEM analysis (Figure S12). The CO_2 evolutions during the acetone photocatalysis under 365 nm monochromic light illumination are shown in Figure S13A,B for the samples with different loading amounts and sizes of Au nanoparticles, respectively, based on which, the CO_2 evolution rates are shown in Figure 15A,B for clear comparison. It is seen that the photocatalytic activity of TiO_2 decreases with the Au/Ti ratio; this is due to that the increase in the Au/TiO_2 perimeter might increase the O_2 sorption-assisted recombination as the Au nanoparticle amount increases. Figure 15B shows that the photocatalytic activity of all Au/TiO_2 samples with different Au nanoparticle sizes is lower than that of pure TiO_2. When the post-annealing temperature was increased from 350 to 450 °C, the increase of photocatalytic activity might be ascribed to that decrease in the Au/TiO_2 perimeter due to the increase of Au size. Although the increase of post-annealing temperature to 550 °C can decrease the Au/TiO_2 perimeter by the further increase of Au size, the decrease of photocatalytic activity may be caused by the decrease in the number of Au nanoparticles that can trap photoinduced electrons.

Contrary to our observation, it has been reported that the Au deposition could increase the photocatalytic oxidation of formaldehyde and acetaldehyde over TiO_2.[42,43] It was thought by us that formaldehyde and acetaldehyde might be adsorbed on the Au/TiO_2 perimeter and react with the photoinduced holes, which could possibly prohibit the recombination via the photoassisted O_2 adsorption−desorption cycling. In addition, we also thought that this result might be different in aqueous photocatalysis, because the resulting O_2^- radicals might diffuse to aqueous solution and are then spatially separated from the
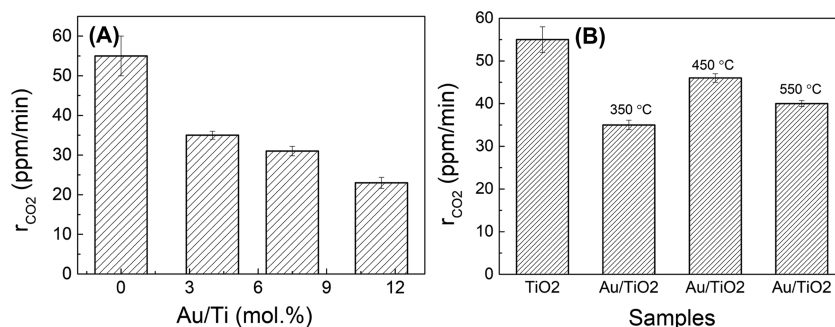
Figure 15. (A) CO_2 evolution rates of the pure TiO_2 and Au/TiO_2 samples with different Au loading amounts. (B) CO_2 evolutions rates of the pure TiO_2 and Au/TiO_2 samples with different Au nanoparticle sizes.

holes. This therefore might inhibit the recombination mediated by O_2 adsorption−desorption cycling. For example, in our previous research, we studied the effect of Au deposition on the photocatalytic degradation of methyl orange over TiO_2 nanorod arrays and it was shown that the photocatalytic activity could be increased.[4]

4. CONCLUSIONS

By means of photoconductance analyses, we revealed that the electron transfer from TiO_2 to O_2 cannot play a crucial role in limiting the acetone photocatalysis. In addition to the photocatalytic effect, it was shown that the electron transfer from TiO_2 to O_2 also contributes to the recombination via O_2-photoassisted adsorption−desorption cycling. It was also revealed that the Au could indeed lead to a great decrease in the E_{app} of electron transfer and accordingly an increase in the electron transfer rate as compared to the pure TiO_2. This however could not result in an increase but a decrease in the acetone photocatalysis over all studied temperatures. Our results indicate a point that the Au-induced increase of electron transfer might increase the recombination via the photoassisted O_2 adsorption−desorption cycling, accordingly reducing the activity of acetone photocatalysis. It indicated that the Au/TiO_2 perimeter might favor the accumulation of photoinduced holes. These holes cannot be captured by acetone, so they contribute to the fast recombination with the photoinduced electrons stored on Au. Because the O_2 photoassisted adsorption−desorption mediated recombination has been assumed to exist in many photocatalysis, a mere increase of the kinetics of electron transfer does not mean an increase in photocatalytic activity if this recombination cannot be inhibited.

ASSOCIATED CONTENT

AUTHOR INFORMATION

Corresponding Author
*E-mail: liubaoshun@126.com.
ORCID
Baoshun Liu: 0000-0001-5564-3685

Xiujian Zhao: 0000-0002-2517-2605

Notes

ACKNOWLEDGMENTS

REFERENCES

(1) Fujishima, A.; Honda, K. Electrochemical Photolysis of Water at a Semiconductor Electrode. *Nature* **1972**, *238*, 37−38.

(2) Huang, H.; Xu, Y.; Feng, Q.; Leung, D. Y. C. Low Temperature Catalytic Oxidation of Volatile Organic Compounds: a Review. *Catal. Sci. Technol.* **2015**, *5*, 2649−2669.

(3) Wang, J.; Liu, B.; Nakata, K. Effects of Crystallinity, {001}/{101} Ratio, and Au Decoration on the Photocatalytic Activity of Anatase TiO_2 Crystals. *Chin. J. Catal.* **2019**, *40*, 403−412.

(4) Chen, J.; Li, Y.; Fang, S.; Yang, Y.; Zhao, X. UV−Vis-infrared Light-driven Thermocatalytic Abatement of Benzene on Fe Doped OMS-2 Nanorods Enhanced by a Novel Photoactivation. *Chem. Eng. J.* **2018**, *332*, 205−215.

(5) Liu, B.; Cheng, K.; Nie, S.; Zhao, X.; Yu, H.; Yu, J.; Fujishima, A.; Nakata, K. Ice−Water Quenching Induced Ti^{3+} Self-doped TiO_2 with Surface Lattice Distortion and the Increased Photocatalytic Activity. *J. Phys. Chem. C* **2017**, *121*, 19836−19848.

(6) Liu, B.; Yan, L.; Wang, J. Liquid N_2 Quenching Induced Oxygen Defects and Surface Distortion in TiO_2 and the Effect on the Photocatalysis of Methylene Blue and Acetone. *Appl. Surf. Sci.* **2019**, *494*, 266−274.

(7) Nakata, K.; Fujishima, A. TiO_2 Photocatalysis: Design and Applications. *J. Photochem. Photobiol., C* **2012**, *13*, 169−189.

(8) Liu, B.; Zhao, X.; Terashima, C.; Fujishima, A.; Nakata, K. Thermodynamic and Kinetic Analysis of Heterogeneous Photocatalysis for Semiconductor Systems. *Phys. Chem. Chem. Phys.* **2014**, *16*, 8751−8760.

(9) Park, H.; Kim, H.; Moon, G.; Choi, W. Photoinduced Charge Transfer Processes in Solar Photocatalysis Based on Modified TiO_2. *Energy Environ. Sci.* **2016**, *9*, 411−433.

(10) Petrik, N. G.; Kimmel, G. A. Electron- and Hole-Mediated Reactions in UV-Irradiated O_2 Adsorbed on Reduced Rutile TiO_2 (110). *J. Phys. Chem. C* **2011**, *115*, 152−164.

(11) Petrik, N. G.; Kimmel, G. A. Photoinduced Dissociation of O_2 on Rutile TiO_2 (110). *J. Phys. Chem. Lett.* **2010**, *1*, 1758−1762.

(12) Nosaka, Y.; Nosaka, A. Y. Generation and Detection of Reactive Oxygen Species in Photocatalysis. *Chem. Rev.* **2017**, *117*, 11302−11336.

(13) Gerischer, H.; Heller, A. The Role of Oxygen in Photooxidation of Organic Molecules on Semiconductor Particles. *J. Phys. Chem.* **1991**, *95*, 5261−5267.

(14) Muggli, D. S.; Falconer, J. L. Role of Lattice Oxygen in Photocatalytic Oxidation on TiO_2. *J. Catal.* **2000**, *191*, 318−325.

(15) Muggli, D. S.; Keyser, S. A.; Falconer, J. L. Photocatalytic Decomposition of Acetic Acid on TiO_2. *Catal. Lett.* **1998**, *55*, 129−132.

(16) Daimon, T.; Hirakawa, T.; Kitazawa, M.; Suetake, J.; Nosaka, Y. Formation of Singlet Molecular Oxygen Associated with the Formation of Superoxide Radicals in Aqueous Suspensions of TiO_2 Photocatalysts. *Appl. Catal., A* **2008**, *340*, 169−175.

(17) Fei, H.; Leng, W.; Li, X.; Cheng, X.; Xu, Y.; Zhang, J.; Cao, C. Photocatalytic Oxidation of Arsenite over TiO_2: Is Superoxide the Main Oxidant in Normal Air-Saturated Aqueous Solutions? *Environ. Sci. Technol.* **2011**, *45*, 4532−4539.

(18) Schneider, J.; Matsuoka, M.; Takeuchi, M.; Zhang, J.; Horiuchi, Y.; Anpo, M.; Bahnemann, D. W. Understanding TiO_2 Photocatalysis: Mechanisms and Materials. *Chem. Rev.* **2014**, *114*, 9919−9986.

(19) Liu, B.; Zhao, X.; Yu, J.; Parkin, I. P.; Fujishima, A.; Nakata, K. Intrinsic Intermediate Gap States of TiO_2 Materials and Their roles in Charge Carrier Kinetic. *J. Photochem. Photobiol., C* **2019**, *39*, 1−57.

(20) Li, X.; Yu, J.; Jaroniec, M.; Chen, X. Cocatalysts for Selective Photoreduction of CO_2 into Solar Fuels. *Chem. Rev.* **2019**, *119*, 3962−4179.

(21) Meng, A.; Wu, S.; Cheng, B.; Yu, J.; Xu, J. Hierarchical TiO_2/$Ni(OH)_2$ Composite Fibers with Enhanced Photocatalytic CO_2 Reduction Performance. *J. Mater. Chem. A* **2018**, *6*, 4729−4736.

(22) Ouyang, W.; Muñoz-Batista, M. J.; Kubacka, A.; Luque, R.; Fernández-García, M. Enhancing Photocatalytic Performance of TiO_2 in H_2 Evolution via Ru Co-catalyst Deposition. *Appl. Catal., B* **2018**, *238*, 434−443.

(23) Hejazi, S.; Altomare, M.; Nguyen, N. T.; Mohajernia, S.; Licklederer, M.; Schmuki, P. Intrinsic Au-decoration on Anodic TiO_2 Nanotubes Grown from Metastable Ti−Au Sputtered Alloys—High Density Co-catalyst Decoration Enhances the Photocatalytic H_2 Evolution. *Appl. Mater. Today* **2019**, *14*, 118−125.

(24) Meng, A.; Zhang, L.; Cheng, B.; Yu, J. Dual Co-catalysts in TiO_2 Photocatalysis. *Adv. Mater.* **2019**, 1807660.

(25) Liu, B.; Nakata, K.; Zhao, X.; Ochiai, T.; Murakami, T.; Fujishima, A. Theoretical Kinetic Analysis of Heterogeneous Photo-catalysis: The Effects of Surface Trapping and Bulk Recombination through Defects. *J. Phys. Chem. C* **2011**, *115*, 16037−16042.

(26) Hou, L.; Zhang, M.; Guan, Z.; Li, Q.; Yang, J. Effect of Annealing Ambience on the Formation of Surface/Bulk Oxygen Vacancies in TiO_2 for Photocatalytic Hydrogen Evolution. *Appl. Surf. Sci.* **2018**, *428*, 640−647.

(27) Yu, X.; Kim, B.; Kim, Y. K. Highly Enhanced Photoactivity of Anatase TiO_2 Nanocrystals by Controlled Hydrogenation-Induced Surface Defects. *ACS Catal.* **2013**, *3*, 2479−2486.

(28) Liu, B.; Wang, J.; Yang, J.; Zhao, X. Charge Carrier Interfacial Transfer Pathways from TiO_2 and Au/TiO_2 Nanorod Arrays to Electrolyte and the Association with Photocatalysis. *Appl. Surf. Sci.* **2019**, *464*, 367−375.

(29) Amano, F.; Nakata, M.; Yamamoto, A.; Tanaka, T. Effect of Ti^{3+} Ions and Conduction Band Electrons on Photocatalytic and Photoelectrochemical Activity of Rutile Titania for Water Oxidation. *J. Phys. Chem. C* **2016**, *120*, 6467−6474.

(30) Kong, M.; Li, Y.; Chen, X.; Tian, T.; Fang, P.; Zheng, F.; Zhao, X. Tuning the Relative Concentration Ratio of Bulk Defects to Surface Defects in TiO_2 Nanocrystals Leads to High Photocatalytic Efficiency. *J. Am. Chem. Soc.* **2011**, *133*, 16414−16417.

(31) Li, Y.; Wang, C.; Zheng, H.; Wan, F.; Yu, F.; Zhang, X.; Liu, Y. Surface Oxygen Vacancies on WO_3 Contributed to Enhanced Photothermo-synergistic Effect. *Appl. Surf. Sci.* **2017**, *391*, 654−661.

(32) Wang, C.; Zhang, X.; Liu, Y. Promotion of Multi-Electron Transfer for Enhanced Photocatalysis: A Review Focused on Oxygen Reduction Reaction. *Appl. Surf. Sci.* **2015**, *358*, 28−45.

(33) Kong, L.; Zhang, X.; Wang, C.; Wan, F.; Li, L. Synergic Effects of Cu_xO Electron Transfer Co-catalyst and Valence Band Edge Control Over TiO_2 for Efficient Visible-Light Photocatalysis. *Chin. J. Catal.* **2017**, *38*, 2120−2131.

(34) Miyauchi, M.; Irie, H.; Liu, M.; Qiu, X.; Yu, H.; Sunada, K.; Hashimoto, K. Visible-Light-Sensitive Photocatalysts: Nanocluster-Grafted Titanium Dioxide for Indoor Environmental Remediation. *J. Phys. Chem. Lett.* **2016**, *7*, 75−84.

(35) Disdier, J.; Herrmann, J. M.; Pichat, P. A Photoconductivity Study of Electron Transfer from the Ultraviolet-illuminated Support to the Metal and of the Influence of Hydrogen. *J. Chem. Soc., Faraday Trans.* **1983**, *79*, 651−660.

(36) Kennedy, J. C., III; Datye, A. K. Photothermal Heterogeneous Oxidation of Ethanol over Pt/TiO_2. *J. Catal.* **1998**, *179*, 375−389.

(37) Panayotov, D. A.; Frenkel, A. I.; Morris, J. R. Catalysis and Photocatalysis by Nanoscale Au/TiO_2: Perspectives for Renewable Energy. *ACS Energy Lett.* **2017**, *2*, 1223−1231.

(38) Zhang, Y.; He, S.; Guo, W.; Hu, Y.; Huang, J.; Mulcahy, J. R.; We, W. D. Surface-Plasmon-Driven Hot Electron Photochemistry. *Chem. Rev.* **2018**, *118*, 2927−2954.

(39) DuChene, J. S.; Sweeny, B. C.; Johnston-Peck, A. C.; Su, D.; Stach, E. A.; Wei, W. D. Prolonged Hot Electron Dynamics in Plasmonic-metal/Semiconductor Heterostructures with Implications for Solar Photocatalysis. *Angew. Chem., Int. Ed.* **2014**, *53*, 7887−7891.

(40) Pu, Y.; Wang, G.; Chang, K.; Ling, Y.; Lin, Y.; Fitzmorris, B. C.; Liu, C.-M.; Lu, Y.; Tong, X.; Zhang, J. Z.; Hsu, Y.-J.; Li, Y. Au Nanostructure-Decorated TiO_2 Nanowires Exhibiting Photoactivity Across Entire UV-visible Region for Photoelectrochemical Water Splitting. *Nano Lett.* **2013**, *13*, 3817−3823.

(41) Reichert, R.; Jusys, Z.; Behm, R. J. Au/TiO_2 Photo(electro)-catalysis: The Role of the Au Co-catalyst in Photoelectrochemical Water Splitting and Photocatalytic H_2 Evolution. *J. Phys. Chem. C* **2015**, *119*, 24750−24759.

(42) Yu, J.; Yue, L.; Liu, S.; Huang, B.; Zhang, X. Hydrothermal Preparation and Photocatalytic Activity of Mesoporous Au−TiO_2 Nanocomposite Microspheres. *J. Colloid Interface Sci.* **2009**, *334*, 58−64.

(43) Kowalska, E.; Mahaney, O. O. P.; Abe, R.; Ohtani, B. Visible-light-induced Photocatalysis through Surface Plasmon Excitation of Gold on Titania Surfaces. *Phys. Chem. Chem. Phys.* **2010**, *12*, 2344−2355.

(44) Lia, X.; Ma, X.-Y.; Liu, J.-L.; Sun, Z.-G.; Zhu, B.; Zhu, A.-M. Plasma-promoted Au/TiO_2 Nanocatalysts for Photocatalytic Form-aldehyde Oxidation under Visible-light Irradiation. *Catal. Today* **2019**, *337*, 132−138.

(45) Fiorenza, R.; Bellardita, M.; D'Urso, L.; Compagnini, G.; Palmisano, L.; Scirè, S. Au/TiO_2-CeO_2 Catalysts for Photocatalytic Water Splitting and VOCs Oxidation Reactions. *Catalysts* **2016**, *6*, 121.

(46) Wu, X.-F.; Song, H.-Y.; Yoon, J.-M.; Yu, Y.-T.; Chen, Y.-F. Synthesis of Core−Shell Au@TiO_2 Nanoparticles with Truncated Wedge-Shaped Morphology and Their Photocatalytic Properties. *Langmuir* **2009**, *25*, 6438−6447.

(47) Tan, T. H.; Scott, J.; Ng, Y. H.; Taylor, R. A.; Aguey-Zinsou, K. F.; Amal, R. Understanding Plasmon and Band Gap Photoexcitation Effects on the Thermal-Catalytic Oxidation of Ethanol by TiO_2-Supported Gold. *ACS Catal.* **2016**, *6*, 1870−1879.

(48) Tamaki, Y.; Hara, K.; Katoh, R.; Tachiya, M.; Furube, A. Femtosecond Visible-to-IR Spectroscopy of TiO_2 Nanocrystalline Films: Elucidation of the Electron Mobility before Deep Trapping. *J. Phys. Chem. C* **2009**, *113*, 11741−11746.

(49) Zhang, S.; Xie, C.; Zhang, G.; Zhu, Q.; Zhang, S. Assessing Multi-variable Coupling Effects of UV Illumination, Heat and Oxygen on Porous ZnO Nanocrystalline Film Through Electron Concen-tration and Mobility Extraction. *Phys. Chem. Chem. Phys.* **2015**, *17*, 18045−18054.

(50) Muraoka, Y.; Takubo, N.; Hiroi, Z. Photoinduced Conductivity in Tin Dioxide Thin Films. *J. Appl. Phys.* **2009**, *105*, 103702.

(51) Herrmann, J. M.; Disdier, J.; Mozzanega, M.-N.; Pichat, P. Heterogeneous Photocatalysis: In Situ Photoconductivity Study of TiO_2 during Oxidation of isobutane into Acetone. *J. Catal.* **1979**, *60*, 369−377.

(52) Golego, N.; Studenikin, S. A.; Cocivera, M. Effect of Oxygen on Transient Photoconductivity in Thin-film $Nb_xTi_{1-x}O_2$. *Phys. Rev. B* **2000**, *61*, 8262−8269.

(53) Golego, N.; Studenikin, S. A.; Cocivera, M. Spray Pyrolysis Preparation of Porous Polycrystalline Thin Films of Titanium Dioxide Containing Li and Nb. *J. Mater. Res.* **1999**, *14*, 698−707.

(54) Navio, J. A.; Coldn, G.; Herrmann, J. M. Photoconductive and Photocatalytic Properties of $ZrTiO_4$. Comparison with the Parent Oxides TiO/and ZrO_2. *J. Photochem. Photobiol., A* **1997**, *108*, 179−185.

(55) Xiao-e, L.; Green, A. N.; Haque, S. A.; Mills, A.; Durrant, J. R. Light-driven Oxygen Scavenging by Titania/polymer Nanocomposite Films. *J. Photochem. Photobiol., A* **2004**, *162*, 253−259.

(56) Liu, B.; Yang, J.; Zhao, X.; Yu, J. The Role of Electron Interfacial Transfer in Mesoporous Nano-TiO_2 Photocatalysis: a Combined Study of in-situ Photoconductivity and Numerical Kinetic Simulation. *Phys. Chem. Chem. Phys.* **2017**, *19*, 8866−8873.

(57) Li, F. F.; Selloni, A. Theoretical Study of Interfacial Electron Transfer from Reduced Anatase $TiO_2(101)$ to Adsorbed O_2. *J. Am. Chem. Soc.* **2013**, *135*, 9195−9199.

(58) Lira, E.; Wendt, S.; Huo, J.; Hansen, J.; Streber, R.; Porsgaard, S.; Wei, Y.; Bechstein, R.; Lægsgaard, E.; Besenbacher, F. The Importance of Bulk Ti^{3+} Defects in the Oxygen Chemistry on Titania Surfaces. *J. Am. Chem. Soc.* **2011**, *133*, 6529−6532.

(59) Larson, S. A.; Widegren, J. A.; Falconer, J. L. Transient Studies of 2-Propanol Photocatalytic Oxidation on Titania. *J. Catal.* **1995**, *157*, 611−625.

(60) Tamaki, Y.; Furube, A.; Murai, M.; Hara, K.; Katoh, R.; Tachiya, M. Direct Observation of Reactive Trapped Holes in TiO_2 Undergoing Photocatalytic Oxidation of Adsorbed Alcohols: Evaluation of the Reaction Rates and Yields. *J. Am. Chem. Soc.* **2006**, *128*, 416−417.

(61) Tachikawa, T.; Majima, T. Single-Molecule Fluorescence Imaging of TiO_2 Photocatalytic Reactions. *Langmuir* **2009**, *25*, 7791−7802.

(62) Tan, H.; Scott, J. A.; Ng, Y. H.; Taylor, R. A.; Aguey-Zinsou, K.-F.; Amal, R. Plasmon Enhanced Selective Electronic Pathways in TiO_2 Supported Atomically Ordered Bimetallic Au-Cu Alloys. *J. Catal.* **2017**, *352*, 638−648.

(63) Zhu, X.; Jin, C.; Li, X.-S.; Liu, J.-L.; Sun, Z.-G.; Shi, C.; Li, X.; Zhu, A.-M. Photocatalytic Formaldehyde Oxidation over Plasmonic Au/TiO_2 under Visible Light: Moisture Indispensability and Light Enhancement. *ACS Catal.* **2017**, *7*, 6514−6524.

(64) Wang, S.; Gao, Y.; Miao, S.; Liu, T.; Mu, L.; Li, R.; Fan, F.; Li, C. Positioning the Water Oxidation Reaction Sites in Plasmonic Photocatalysts. *J. Am. Chem. Soc.* **2017**, *139*, 11771−11778.